






ORIGINAL ARTICLE

In vivo multiphoton imaging for non-invasive time course assessment of retinoids effects on human skin

Emmanuelle Tancrède-Bohin^{1,2}  | Thérèse Baldeweck³ | Sébastien Brizion³  |
Etienne Decencièrè⁴  | Steeve Victorin³ | Blandine Ngo³ | Edouard Raynaud³ |
Luc Souverain³ | Martine Bagot^{2,5}  | Ana-Maria Pena³ 

¹L'Oréal Research and Innovation, Clichy, France

²Service de Dermatologie, Hôpital Saint-Louis, Paris, France

³L'Oréal Research and Innovation, Aulnay-sous-Bois, France

⁴Center for Mathematical Morphology, MINES ParisTech – PSL Research University, Fontainebleau, France

⁵Inserm U976, Hôpital Saint-Louis, Université de Paris, Paris, France

Correspondence

Emmanuelle Tancrède-Bohin, L'Oréal Research and Innovation, Campus Charles Zviak RIO, 9 rue Pierre Dreyfus, Clichy, France.

Email: emmanuelle.tancrede-bohin@rd.loreal.com

Abstract

Background: In vivo multiphoton imaging and automatic 3D image processing tools provide quantitative information on human skin constituents. These multiphoton-based tools allowed evidencing retinoids epidermal effects in the occlusive patch test protocol developed for antiaging products screening. This study aimed at investigating their relevance for non-invasive, time course assessment of retinoids cutaneous effects under real-life conditions for one year.

Materials and Methods: Thirty women, 55-65 y, applied either retinol (RO 0.3%) or retinoic acid (RA 0.025%) on one forearm dorsal side versus a control product on the other forearm once a day for 1 year. In vivo multiphoton imaging was performed every three months, and biopsies were taken after 1 year. Epidermal thickness and dermal-epidermal junction undulation were estimated in 3D with multiphoton and in 2D with histology, whereas global melanin density and its z-epidermal distribution were estimated using 3D multiphoton image processing tools.

Results: Main results after one year were as follows: a) epidermal thickening with RO (+30%); b) slight increase in dermal-epidermal junction undulation with RO; c) slight decrease in 3D melanin density with RA; d) limitation of the melanin ascent observed with seasonality and time within supra-basal layers with both retinoids, using multiphoton 3D-melanin z-epidermal profile.

Conclusions: With a novel 3D descriptor of melanin z-epidermal distribution, in vivo multiphoton imaging allows demonstrating that daily usage of retinoids counteracts aging by acting not only on epidermal morphology, but also on melanin that is shown to accumulate in the supra-basal layers with time.

KEYWORDS

aging, fluorescence lifetime imaging, human skin, melanin, pigmentation, retinoic acid, retinol, two-photon excited fluorescence

Baldeweck and Pena contributed equally to this work

This is an open access article under the terms of the Creative Commons Attribution-NonCommercial-NoDerivs License, which permits use and distribution in any medium, provided the original work is properly cited, the use is non-commercial and no modifications or adaptations are made.

© 2020 The Authors. *Skin Research and Technology* published by John Wiley & Sons Ltd

1 | INTRODUCTION

In dermatological clinical research, *in vivo* multiphoton microscopy^{1,2} offers the possibility to avoid invasive biopsies and to supply information on the skin state before, during and after a cutaneous treatment. Epidermis and superficial dermis can be characterized with sub-micrometer resolution up to ~160-200 μm depth, by taking advantage of intrinsic multiphoton signals: second-harmonic generation (SHG) created by fibrillar collagens and two-photon excited fluorescence (2PEF) emitted by keratin, nicotinamide adenine dinucleotide, flavin adenine dinucleotide, melanin, or elastin.³

The advent of medically approved multiphoton microscopes⁴ enabled a broad range of clinical applications spanning from the characterization of human skin pigmentation,^{3,5,6} age-related, or photoaging changes,⁷⁻¹² dermatological disorders and melanoma¹³⁻²¹ up to the assessment of penetration and effects of pharmaceutical/ cosmetic products on human skin.^{3,12,22-28}

Multiphoton images of *in vivo* human skin contain a lot of valuable information that can be extracted using appropriate image processing tools. We recently developed the first 3D image processing tools allowing an automatic segmentation of the different skin layers and the extraction of several quantitative parameters.^{6,10} For example, epidermal thickness, melanin content, or the dermal-epidermal junction (DEJ) shape can be quantified in 3D. Using these tools, we validated several quantitative parameters of interest for studying photoaging process, constitutive pigmentation, or whitening phenomena^{3,8,10} and demonstrated that multiphoton-based methods allowed epidermal effects induced by RO and RA to be accurately and non-invasively detected and quantified in the occlusive patch test protocol developed for antiaging products screening.²⁶ However, this model is not truly representative of the real-life situation as occlusion produces effects by itself and of course enhances pharmacological penetration.

The present study aimed at investigating the relevance of *in vivo* multiphoton imaging for the assessment of RO and RA cutaneous effects over one year, under real-life conditions, and at calibrating the variation amplitude of multiphoton quantification parameters with these antiaging gold standards.

2 | MATERIALS AND METHODS

2.1 | Subjects and treatment

This study involved 30 healthy European women aged 50-65y with photodamaged skin and a dorsal forearm skin color with ITA value between 10° and 41° (skin color group tanned to intermediate). They applied Retinol 0.3% (RO, Retinol 0.3% cream, L'Oréal group) (n = 15) or all-trans-Retinoic acid 0.025% (RA, Retinoic acid 0.025% cream, Galderma) (n = 15) on one dorsal forearm versus a control product (white paraffin containing excipient, Bayer) on the other forearm for 1 year, with an every other day application during the first month

followed by a daily application for the rest of the study. Additionally, during summer, volunteers were advised to avoid sun exposure, to wear covering sleeves and use a provided sunscreen SPF 50 when exposure to sun was unavoidable. A randomization list, generated by an unblinded data management person, determined the product nature to be applied on the left or right forearm for all volunteers and the study was double-blinded, that is, neither investigator nor volunteers knew the product's nature on each arm.

The study was conducted in Paris, France (February 2011-April 2012). Evaluations were performed on the same area at months M00 (March), M03 (June), M06 (September), and M12 (March + 1 year) using multiphoton and colorimetric measurements. Areas of investigation were identified by tracing on transparent plastic sheets (Monaderm, Monaco) natural anatomic marks (external and internal forearm edges, ulna head, elbow fold) and also skin folds and nevus on volunteers in a standardized position. At M12, biopsies were taken for histological analysis. Possible cutaneous irritation was followed up by a dermatologist at each visit. Recourse to an every other day application after the first month was allowed if necessary to obtain an acceptable tolerance.

The study was conducted in accordance to the Declaration of Helsinki principles, approved by Saint-Louis Hospital Ethics Committee, and all volunteers gave written, informed consent (EC reference 2010/58).

2.2 | Multiphoton imaging and 3D image processing

Multiphoton imaging was performed with Dermalinspect™ (JenLab GmbH, Jena, Germany), as previously described.^{25,26} For each treated area, we acquired two adjacent 3D-xyz images (z-stacks of 70 *en face* 2PEF/SHG images of 511x511 pixels (0.25 μm /pixel) acquired with 2.35 μm z-step upon 760 nm excitation). The 2 z-stacks were acquired within the same central part of the 0.8 cm^2 delimited region over time.

The z-stacks were quantified using automatic 3D image processing tools^{6,10} to identify the skin layers, characterize the DEJ 3D-shape, and extract quantitative parameters about the different skin constituents and layers.

The first image processing step consists of an epidermis/ dermis 3D segmentation, taking into account the real shapes of skin surface and DEJ, followed by a 3D epidermis segmentation of SC and LED sub-layers.

The second step comprises the extraction of quantitative parameters. We quantified morphological parameters: SC, LED, and total epidermis mean thickness (measured along the z axis at each (x,y) position and the mean value was computed) and normalized DEJ area characterizing DEJ undulation in 3D (a generalization in 3D of the interdigitation index described in 2D in histology¹⁰). It is expressed as the ratio between the real DEJ area and the area of its projection on a horizontal plane. Hence, flat DEJ leads to a ratio of 1 and more undulated DEJ to values above 1.

Melanin 3D quantification was performed using Pseudo-FLIM approach combining multiphoton microscopy and fluorescence lifetime imaging.^{3,6,12} Melanin density corresponds to the ratio between the number of melanin voxels to the number of epidermal voxels. The epidermal melanin density z-distribution (z-profile of melanin density in 12 thickness-normalized epidermal layers from 1 - DEJ level to 12 - SC level) was computed and examples of z-profiles, corresponding raw 2PEF images and melanin masks are shown in Figure 1.

2.3 | Colorimetry

Skin color was determined by the ITA values using a microflash spectroradiometer (Datacolor, Montreuil, France) that was calibrated before each measurement.

2.4 | Histology

Two biopsies were collected per volunteer at M12, one on each forearm. Cryostat sections were processed for light microscopy (NIKON E400) and stained with HES for overall morphological evaluation, Fontana-Masson, Luna'aldehyde fuchsin, and Sirius red for melanin, elastic fibers, and collagen visualization respectively. All measurements were performed using ImageJ (W. Rasband, NIH, USA). Measurements of 2D epidermal thickness were taken from the DEJ to the SC surface along the entire section length, and the mean thickness calculated. The 2D interdigitation index,²⁹ characterizing DEJ undulation, was calculated as the ratio between the lengths of basal membrane and *stratum lucidum*, with values closed to 1 revealing a flat DEJ. Quantification of melanin, elastic fibers, and collagen 2D densities correspond to the ratio between the colored surface and the total surface of the epidermis (melanin) or dermis (elastic fibers and collagen).

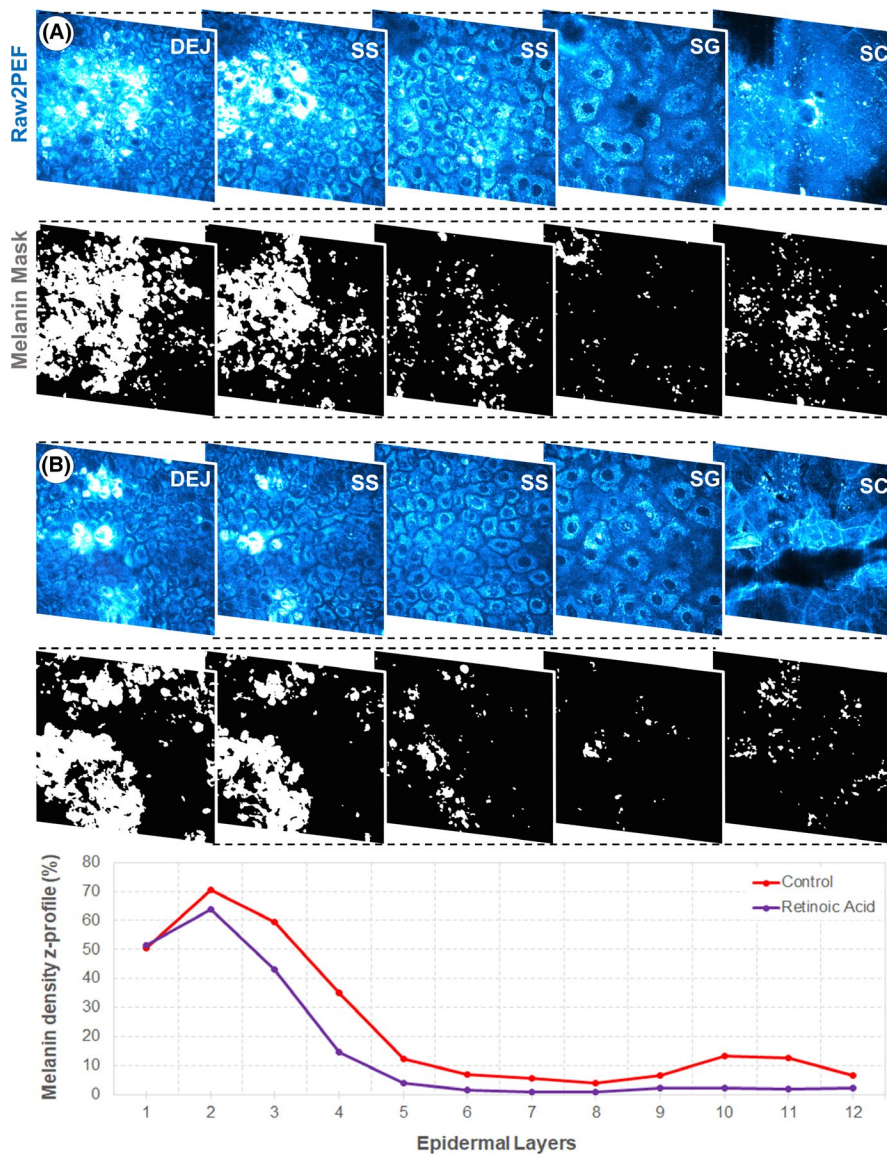


FIGURE 1 Pseudo-FLIM melanin quantification and melanin density z-profile. (top) Examples of in vivo 2PEF raw multiphoton images (cyan hot color) with corresponding melanin masks, obtained after image processing using Pseudo-FLIM approach, at different depths within the epidermis of A) control and B) retinoic acid-treated skin at M12. (bottom) Corresponding melanin z-epidermal distribution profiles (melanin density in 12 thickness-normalized epidermal layers from 1—DEJ level to 12—SC level). SC—*stratum corneum*, SG—*stratum granulosum*, SS—*stratum spinosum*, DEJ—dermal-epidermal junction [Colour figure can be viewed at wileyonlinelibrary.com]

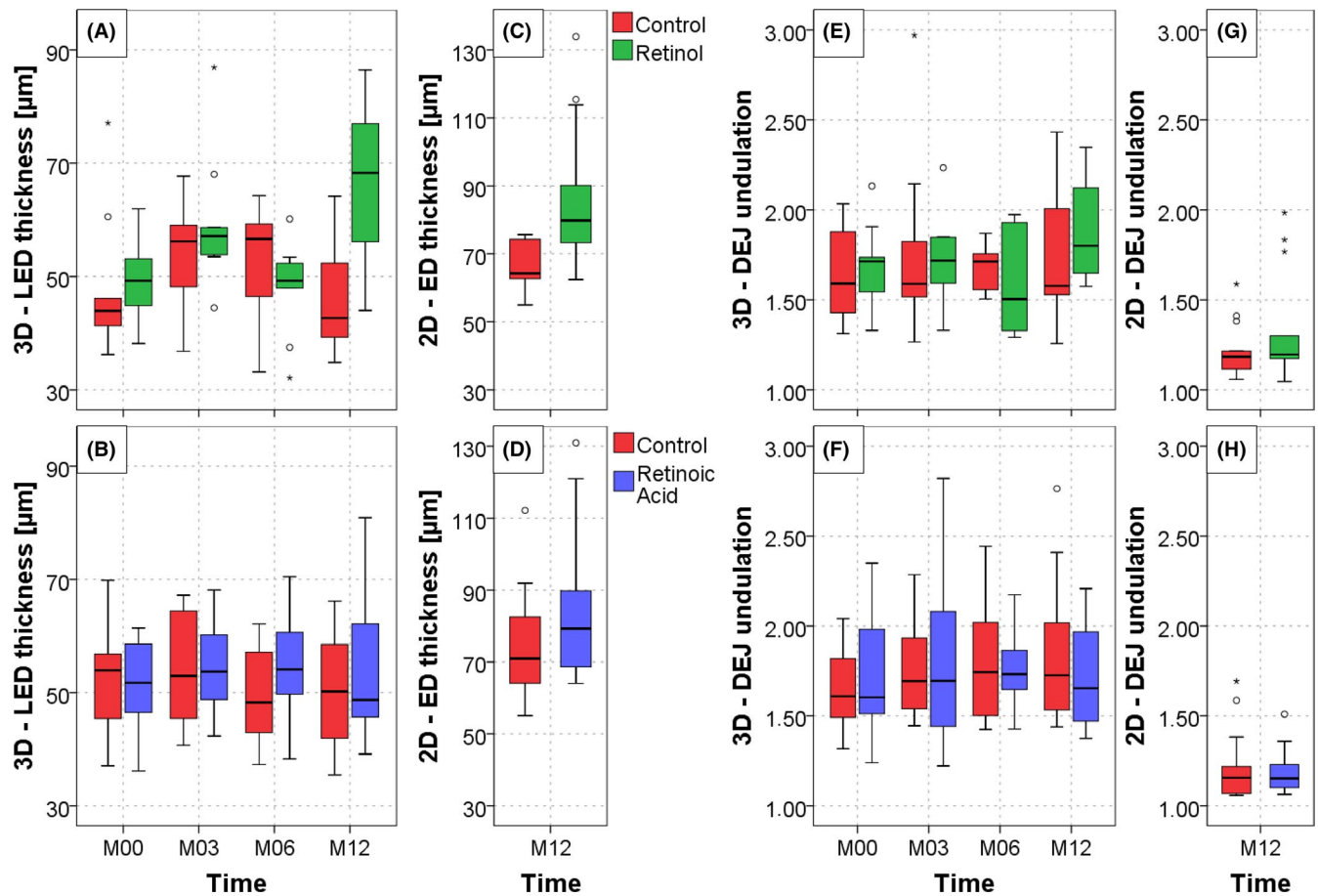


FIGURE 2 Multiphoton and histology quantification results of retinol 0.3% and retinoic acid 0.025% effects on epidermis thickness and dermal-epidermal junction undulation over one year. (A, B) Living epidermis thickness measured in 3D by multiphoton microscopy; (C, D) epidermis thickness measured in 2D by histology; (E, F) DEJ undulation measured in 3D by multiphoton microscopy; (G, H) DEJ undulation measured in 2D by histology. No unit (ratios), both parameters equal to 1 for a totally flat DEJ and >1 for a more undulated junction (see Materials and methods section). The data are expressed as box plots with fences [Colour figure can be viewed at wileyonlinelibrary.com]

2.5 | Statistical methods

For each parameter, changes from baseline were analyzed using R. Data distributions were described for each parameter using box plots.

Results have been interpreted using both effect size (ES) and inferential analysis as currently recommended.³⁰ ES represents the difference of means between groups compared to the variability of the phenomenon and gives an idea of the strength of the modifications observed between groups. The effect size depends only on the underlying population parameters, not on the sample size as the p -value, and allows meaningful comparison between different studies outcomes.

The criteria for ES interpretation of multiphoton and histology parameters have been built from contrasts clearly relevant in the study context²⁶: very strong: $ES > 1.3$; strong: $0.8 < ES < 1.3$; moderate: $0.5 < ES < 0.8$; small: $0.3 < ES < 0.5$; very small: $ES < 0.3$.

For each parameter, the inferential analysis was performed using a linear mixed model for quantitative longitudinal data with treatment, time, and the interaction treatment*time as fixed effects and subject as random. Within and between treatment groups, comparisons were performed using contrasts. Lsd adjustment for p -value tests was used. All hypothesis tests

comparing the treatments were performed using two-sided tests with $\alpha = 0.05$ significance level.

The results are given in the text as estimated mean \pm SEM with strength of ES and P -value (NS if > 0.05) in parentheses.

3 | RESULTS

In this 1-year kinetic study, control, RO- or RA-treated dorsal forearm skin was investigated at M00 (March, before treatment), M03 (June), M06 (September), and M12 (March + 1 year) in thirty 55–65 year women using multiphoton imaging and colorimetry, and at M12 using histology.

3.1 | Quantitation results obtained after 3D image processing of multiphoton images

3.1.1 | Retinoids effects on 3D epidermis thickness

Modifications of living epidermis (LED) and total epidermis (SC + LED) thickness were similar thus only results on LED are

shown (Figure 2A-B). At baseline, the $50 \pm 9 \mu\text{m}$ mean LED thickness showed no difference between the two forearms and remained unchanged for the study duration on control sites in both groups, except at M03 for the RO-control group ($+6.6 \mu\text{m}$; p NS, moderate ES).

On RO-treated sites, a clear increase in mean LED thickness was shown at M03 ($+11.1 \mu\text{m}$, $P = .003$, strong ES) and M12 ($+18.5 \mu\text{m}$, $P < .001$, very strong ES) as compared with M00. At M12, LED thickness increase was also significantly higher compared with control site ($\Delta 20.5 \mu\text{m}$, $P < .001$, very strong ES). The LED thickness increase is illustrated in Figure 3 showing multiphoton images and 3D volume renderings of the segmented epidermal and dermal compartments at M12 on control (Figure 3A) and RO-treated site (Figure 3B) in a representative subject

On RA-treated sites, slight increase in mean LED thickness was observed at M06 and M12, associated with a moderate ES compared to control but was not statistically significant (p NS).

3.1.2 | Retinoids effects on 3D dermal-epidermal junction undulation

At baseline, the mean DEJ normalized area, characterizing DEJ undulation in 3D, was 1.7 ± 0.3 with no difference between the two

forearms and remained unchanged for the study duration on control sites in both groups (Figure 2E-F). On RO-treated sites, the mean value increased to 1.9 ± 0.3 at M12 (p NS, moderate ES as compared to M00 and to control). On RA-treated sites, no modification was observed.

The dermis surface in Figure 3 allows visualizing the DEJ shape, and hence, its undulation, within the $\sim 130 \times 130 \mu\text{m}^2$ field of view.

3.1.3 | Modulation of global epidermal 3D melanin density with seasonality and retinoids

At baseline (Figure 4A), the mean 3D epidermal melanin density was $14 \pm 0.1\%$, with no difference between the two forearms in both groups. At M06, after summer, a clear increase of 9 to 15% is observed, on control and retinoid-treated sites, in both groups as compared to M00 ($P < .005$ with strong to very strong ES for all conditions), with no difference between the control and retinoid-treated sites. At M12, melanin density in the control of RO-group decreased back to M00 level, whereas in the control of RA-group, a persistent increase was observed compared with M00 ($+7\%$ $P = .019$, strong ES). In the treated conditions at M12, melanin density decreased back to M00 level for both treated sites with no difference compared with control in RO-treated sites, but with a

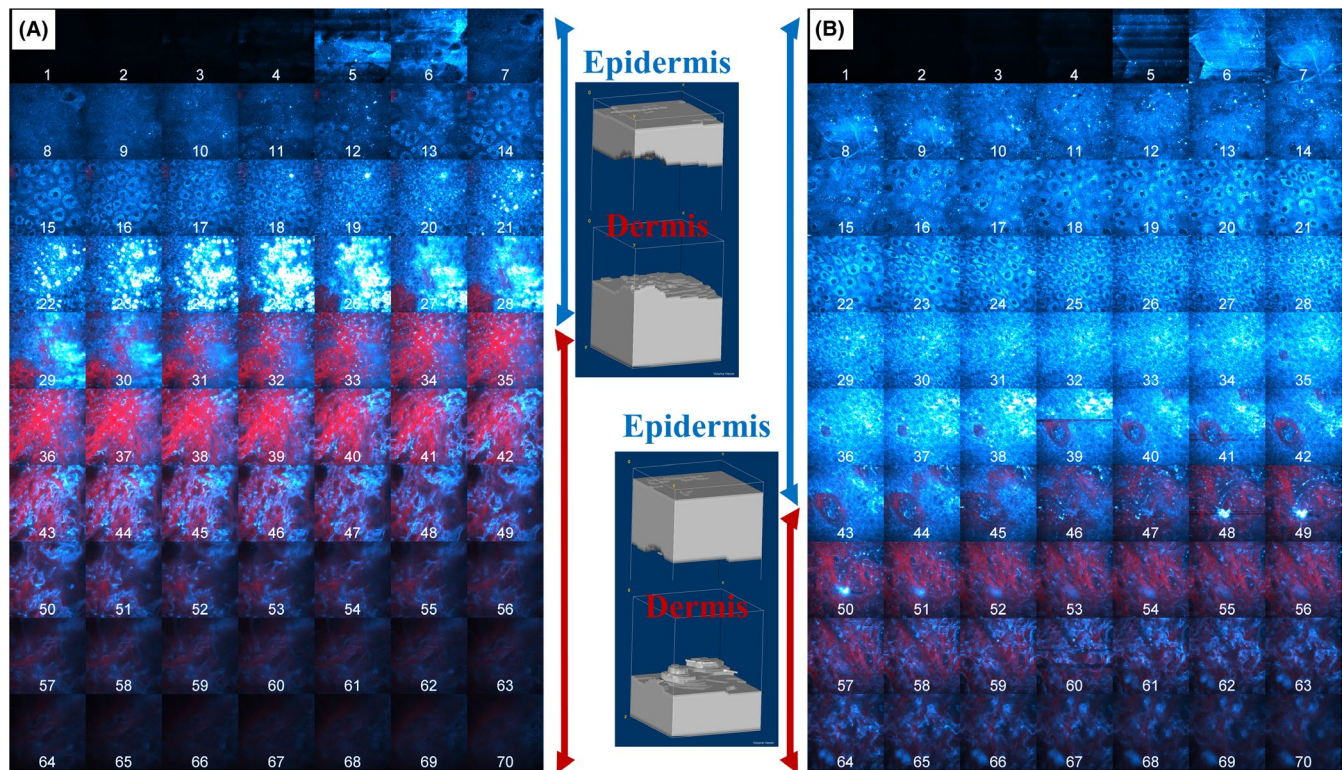
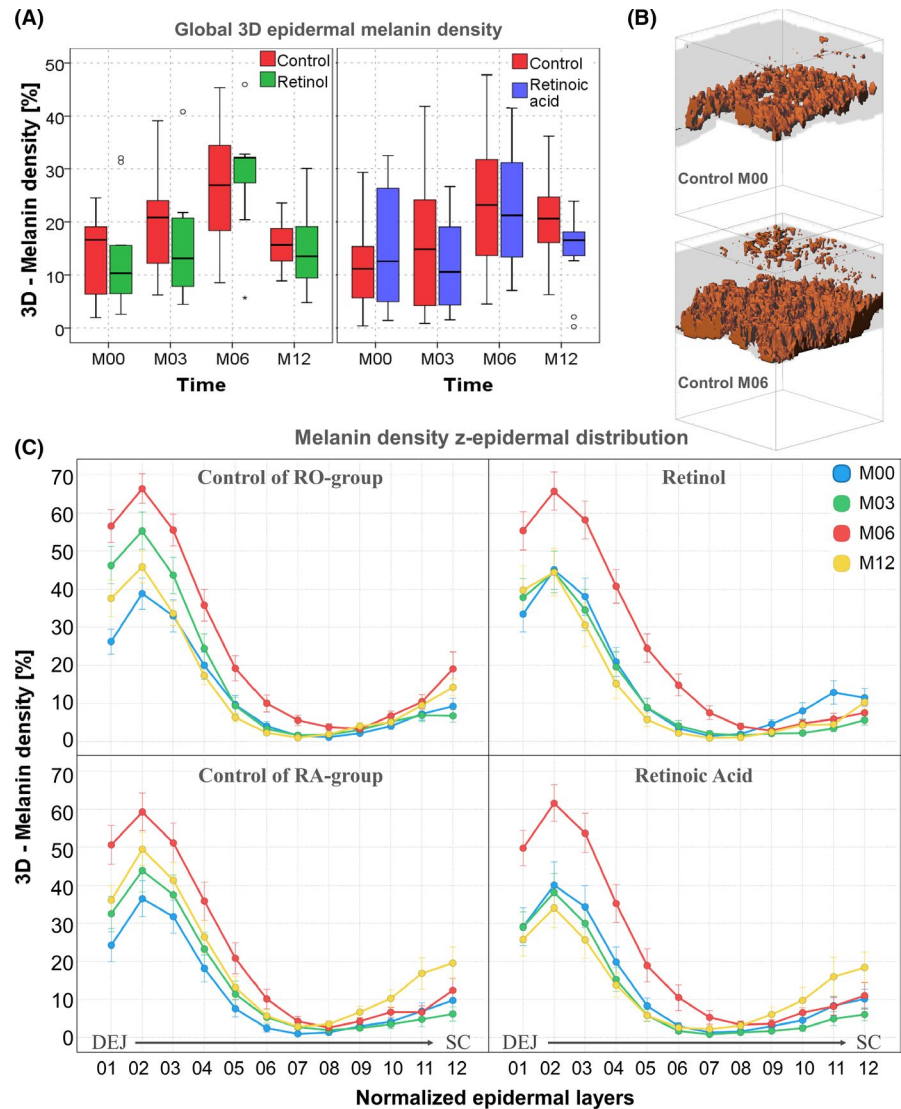


FIGURE 3 In vivo multiphoton images and 3D volume renderings of retinol 0.3% effects at M12. (A) control and (B) RO-treated side in a representative subject. The mosaic images show all the images within a z-stack of combined 2PEF (cyan hot color)/ SHG (red color) images. The images in the middle correspond to their respective 3D volume reconstruction of the segmented epidermal and dermal compartments, obtained using the 3D automatic segmentation method and allowing to visualize epidermis thickness and DEJ shape. The epidermis is depicted as a cyan bracket and the dermis as a red bracket. The 3D volume reconstructions were created using ImageJ software [Colour figure can be viewed at wileyonlinelibrary.com]

FIGURE 4 Modulation of melanin global density and z-epidermal distribution with seasonality and retinoids. A) change with time in the global 3D epidermal melanin density. The data are expressed as box plots with fences. B) 3D melanin masks of a representative control subject at M00 and M06. These 3D reconstructions were created with Imaris (Bitplane AG, Zürich, Switzerland) software; C) Melanin z-epidermal distribution (mean 3D melanin density estimated in 12 thickness-normalized epidermal layers from 1–DEJ level to 12–SC level). The z-profiles data are expressed as mean \pm SEM [Colour figure can be viewed at wileyonlinelibrary.com]



slight difference in RA-treated sites compared with control (-6% , p NS, moderate ES).

3.1.4 | Modulation of 3D melanin z-epidermal distribution with seasonality and retinoids

When dividing the epidermis into several thickness-normalized sub-layers, one can measure the 3D melanin z-epidermal distribution profile and get an insight into melanin content changes appearing within these layers: synthesis within the basal layer or transfer within the upper layers. Depending on the modulation level of this profile, the changes can impact or not the global epidermal 3D melanin density. For example, a decrease in one layer could be counteracted by an increase in another layer, and hence, no change will be evidenced in the global epidermal 3D melanin density. Also, slight modulations not detectable at the global level can be evidenced.

In the control condition (Figure 4C left), analysis of melanin z-epidermal distribution revealed that the gradual increase of global

3D epidermal melanin density is due to an increase in the basal layers, but also up to the middle epidermis at M03, and throughout the epidermis at M06 (after summer). This can also be visualized in Figure 4B, on the M00 and M06 3D melanin masks of a representative control subject. At M12, a persistent accumulation of melanin in the basal and supra-basal layers, as well as at the SC level was observed when compared to M00.

In both retinoid-treated groups (Figure 4C right), the strongest modulation of melanin distribution induced by summer (M06) was not different compared with control group, but the ascent of melanin in the supra-basal layers appearing in control groups was not observed at M03 nor at M12. The z-profile of melanin density at these times overlaps M00 curve for RO-condition and even slightly decreased in the first third of epidermis for RA-condition at M12 consistent with the slight difference in global epidermal melanin density observed at this time.

Examples of multiphoton 2PEF images, melanin masks, and 3D melanin z-epidermal distributions at M12 on control and RA-treated site in a representative subject are given in Figure 1.

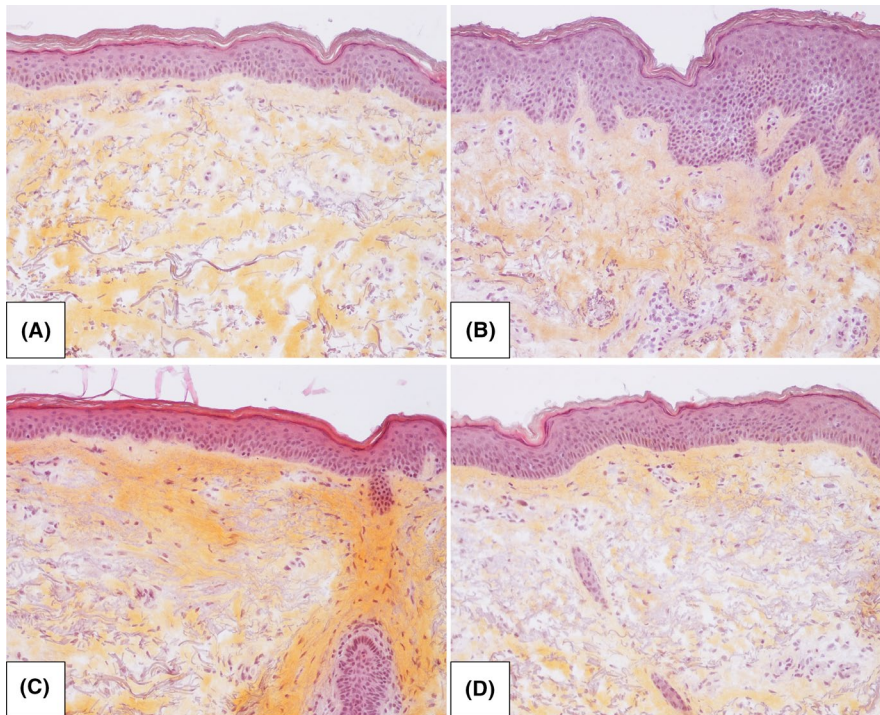


FIGURE 5 Histological photomicrographs of control and retinoid-treated skin in representative subjects at M12. HES (Hematoxylin-eosin stain, x20) images of A) control of RO-group, B) RO-treated skin, C) control of RA-group, and D) RA-treated skin in representative subjects at M12 [Colour figure can be viewed at wileyonlinelibrary.com]

3.2 | Results from histology

At M12, consistent with multiphoton results, quantitative measurements of the HES-stained biopsy skin sections showed following treatment with RO and RA a mean increase in epidermal thickness by 19.6 μm ($P = .002$, very strong ES) and 10.4 μm (p NS, moderate ES) respectively compared with control (Figure 2C-D). The increase in DEJ undulation was not statistically significant but showed a moderate ES on RO-treated site compared with control (Figure 2G-H). Figure 5 shows representative histological photomicrographs of control and retinoid-treated sides at M12. Histological quantification of melanin, elastic fibers, and collagen showed no statistically significant difference between retinoid-treated and control sites at M12 (data not shown).

3.3 | Results from colorimetric measurements

At baseline, the mean ITA value was 38 ± 7 for all conditions and decreased of about 5° at M03 ($P < .015$, moderate ES for all conditions, except RA-treated site p NS, weak ES) and 10° at M06 ($P < .001$, strong to very strong ES), indicating moderate tanning, before increasing to the baseline value again at M12 in all conditions with no differences between them (data not shown).

3.4 | Tolerance

Despite an every other day application during the 1st month, erythema or mild burning or stinging was noted in 14 RO- and in 6 RA-treated volunteers, mostly transient and rated as mild. For 5

subjects, the number of planned applications was reduced and additional every other day application periods prescribed: for 1 month (1RA, 1RO), 4 months (1RO), and for all the study duration (2RO). One subject was released from the study at M06 (RO).

4 | DISCUSSION

Despite its small field of view, long image acquisition time, cost, and the expertise required to master the technology, *in vivo* multiphoton imaging affords quantitative information on human skin constituents with unprecedented specificity. This study confirms the capabilities of multiphoton imaging combined with specific 3D image processing tools for time-course assessment of dermatological/cosmetic treatments. Indeed, in agreement with literature,³¹⁻³⁷ RO and RA are shown to increase epidermal thickness after one year with both 3D-multiphoton and 2D-histological quantifications. Regarding DEJ undulation, we previously reported with multiphoton imaging an increase of this parameter with 0.3% RO in the occlusive patch test.²⁶ In this study, although non-statistically significant, a slight increase is detected with RO, associated with moderate ES with both multiphoton (versus M00 and versus control) and histology (versus control) after 1 year. The beneficial effects on epidermis are here more pronounced with RO than with RA, and this is likely due to the high concentration of RO used (0.3%), 12 times higher compared with RA concentration (0.025%), as in our previous short term study.²⁶

Beside epidermal morphological changes, multiphoton fluorescence lifetime imaging has the unique capacity to specifically detect, quantify, and describe the precise 3D-distribution of melanin in the epidermis.³ The study shows *in vivo* the progressive increase of global 3D-melanin density with summer. It's noteworthy

that the summery modulations of melanin density are quite weak in this study, due to the sun-protection regime prescribed to the volunteers. The instructions were overall respected, as evidenced by a rather low increase of pigmentation in summer as measured by a mean decrease of ITA of 10° which corresponds to the usual difference of color observed between the dorsal and the ventral side of the forearm in winter in healthy subjects of the same age and phototype (personal data).

This study also reveals for the first time, the gradual ascent of melanin from the basal layers into the upper epidermal layers. This melanin z-epidermal distribution allows identifying small changes that are not necessarily detectable or associated to a change at the global level. Indeed, on control sites after one year, this melanin z-profile reveals a persistent melanin in the supra-basal layers, in the first third of epidermis. The same pattern of melanin distribution has also been observed in other studies that compared either, chronically exposed and non-exposed skin in the same subject, or old vs younger subjects on the same chronically photoexposed area at distance of seasonality effect (personal data). Thus, persistent melanin into the supra-basal layers of epidermis could be a new pertinent descriptor of photoaging in Europeans. Its advantage over other photoaging markers is that its modulation is evident over one year, whereas flattening of DEJ or epidermal thinning is not detectable in such a short time frame. Moreover, the improvement seen with gold standard antiaging treatments validates this parameter as a good candidate for further anti-photoaging products evaluation. Indeed, in both retinoid-treated conditions, the progressive ascent at M03 and persistent ascent at M12 in pigmentation, appearing within supra-basal epidermal layers of control groups, are not observed.

This visualization of the modulation of global melanin content and its epidermal distribution under treatment also strongly supports that in vivo, the predominant effect of retinoids on pigmentation is more likely due to skin renewal than to a direct effect on melanogenesis as discussed in literature.³⁸⁻⁴⁰

As already shown,^{8,10} multiphoton imaging also allows investigating human skin up to ~150 µm depth corresponding to approximately 80 µm of superficial dermis in a normal untreated skin. In this study, the biggest proportion of dermis between treated and control skin at every time point was restricted to a 30 µm thick dermal layer below the DEJ. This relates to the mean epidermal thickening of 30% in RO-treated areas, even higher than 50% in a third of volunteers of this group. In these conditions, the superficial dermis was not assessed by multiphoton. After one year, no obvious quantitative change in the dermal fibrillary networks was shown by standard histological assessment in our study. Although retinoids are known to increase expression of type I procollagen^{36,41-43} a direct increase of collagen by retinoids has rarely been demonstrated and a decrease of dermal elastosis has only been observed after up to 4 years therapy.³³ Hence, we believe that changes in the dermis that could be addressed with this technique are not likely to be observed in such study duration.

5 | CONCLUSION

This study shows for the first time that, under real-life conditions, in vivo multiphoton microscopy associated with specific 3D quantification tools allows epidermal effects induced by treatments, including melanin content, to be accurately and non-invasively quantified. In vivo melanin z-epidermal distribution is assessed here for the first time and provides new insights into the knowledge of pigmentation modulation with seasonality and retinoids treatment. Knowing the importance of epidermal melanin distribution for its DNA protection factor,⁴⁴⁻⁴⁶ our new method could be applied to improve the knowledge of some underlying biological mechanisms of pigmentation modulations appearing through either redistribution of existing melanin and/or de novo melanin synthesis. The applications of these multiphoton-based melanin quantification parameters can span from physiological, pathological, or environmental factors-induced pigmentation modulations up to whitening, anti-photoaging, or photoprotection products evaluation.


ACKNOWLEDGEMENTS

The authors gratefully acknowledge Nathalie Parent and Marjorie Carpentier for their help in carrying out the study, Léa Sallé for helping with manuscript preparation and Dr Damilola Fajuyigbe for reviewing the manuscript.

CONFLICT OF INTEREST

TB, SB, BN, AMP, ER, LS, ETB, and SV are employees of L'Oréal Research and Innovation. One of the studied products (Retinol) is commercialized by L'Oréal Group. ED is one of the inventors of the patented 3D image processing tools used in this study. MB has no conflict of interest.

ORCID

Emmanuelle Tancrède-Bohin  <https://orcid.org/0000-0002-0412-0806>

Sébastien Brizion  <https://orcid.org/0000-0003-1454-4204>

Etienne Decencièrre  <https://orcid.org/0000-0002-1349-8042>

Martine Bagot  <https://orcid.org/0000-0002-0400-1954>

Ana-Maria Pena  <https://orcid.org/0000-0001-9943-2513>

REFERENCES

1. So PTC, Yew E, Rowlands C. Chapter 19 - Applications of Multiphoton Microscopy in Dermatology. In: Hamblin MR, Avci P, Gupta GK, eds. *Imaging in Dermatology*. Boston: Academic Press; 2016:241-268.
2. König K. *Multiphoton microscopy and fluorescence lifetime imaging, applications in biology and medicine*. Berlin, Boston: De Gruyter; 2018.
3. Pena A-M, Decencièrre E, Brizion S, et al. Multiphoton FLIM in cosmetic clinical research. In König K, ed. *Multiphoton Microscopy and Fluorescence Lifetime Imaging. Applications in Biology and Medicine*. Berlin, Boston: De Gruyter; 2018:369-393.
4. König K. Hybrid multiphoton multimodal tomography of in vivo human skin. *IntraVital*. 2012;1(1):11-26.
5. Saager RB, Balu M, Crosignani V, et al. In vivo measurements of cutaneous melanin across spatial scales: Using multiphoton microscopy and spatial frequency domain spectroscopy. *J Biomed Opt*. 2015;20(6).

6. Pena A-M, Baldeweck T, Tancrede E, Decencièrre E, Koudoro S. Inventors. Non-invasive method for specific 3D detection, visualization and/or quantification of an endogeneous fluorophore such as melanin in a biological tissue. French patent FR2982369, International publication number WO20130689432011.
7. Koehler MJ, Preller A, Kindler N, et al. Intrinsic, solar and sunbed-induced skin aging measured in vivo by multiphoton laser tomography and biophysical methods. *Skin Res Technol*. 2009;15(3):357-363.
8. Baldeweck T, Tancrede E, Dokladal P, et al. In vivo multiphoton microscopy associated to 3D image processing for human skin characterization. *Progr Biomed Opt Imaging Proc SPIE*. 2012;8226:82263o.
9. Koehler MJ, Preller A, Elsner P, Konig K, Hipler UC, Kaatz M. Non-invasive evaluation of dermal elastosis by in vivo multiphoton tomography with autofluorescence lifetime measurements. *Exp Dermatol*. 2012;21(1):48-51.
10. Decencièrre E, Tancrede-Bohin E, Dokladal P, Koudoro S, Pena AM, Baldeweck T. Automatic 3D segmentation of multiphoton images: A key step for the quantification of human skin. *Skin Res Technol*. 2013;19:115-124.
11. Sanchez WY, Obispo C, Ryan E, Grice JE, Roberts MS. Erratum: Changes in the redox state and endogenous fluorescence of in vivo human skin due to intrinsic and photo-aging, measured by multiphoton tomography with fluorescence lifetime imaging (Journal of Biomedical Optics (2013) 18 (061217)). *J Biomed Opt*. 2013;18(6).
12. Pena AM, Aguilar L, Azadiguan G, et al. Multiphoton imaging in cosmetics research. *Progr Biomed Opt Imaging Proc SPIE*. 2019;10859:1085907.
13. Dimitrow E, Ziemer M, Koehler MJ, et al. Sensitivity and specificity of multiphoton laser tomography for in vivo and ex vivo diagnosis of malignant melanoma. *J Invest Dermatol*. 2009;129(7):1752-1758.
14. Paoli J, Smedh M, Ericson MB. Multiphoton laser scanning microscopy—a novel diagnostic method for superficial skin cancers. *Semin Cutan Med Surg*. 2009;28(3):190-195.
15. Seidenari S, Arginelli F, Bassoli S, et al. Diagnosis of BCC by multiphoton laser tomography. *Skin Res Technol*. 2013;19(1):e297-e304.
16. Patalay R, Talbot C, Alexandrov Y, et al. Multiphoton multispectral fluorescence lifetime tomography for the evaluation of basal cell carcinomas. *PLoS One*. 2012;7(9):e43460.
17. Ulrich M, Klemp M, Darwin ME, Konig K, Lademann J, Meinke MC. In vivo detection of basal cell carcinoma: comparison of a reflectance confocal microscope and a multiphoton tomograph. *J Biomed Opt*. 2013;18(6):61229.
18. Balu M, Kelly KM, Zachary CB, et al. Distinguishing between benign and malignant melanocytic nevi by in vivo multiphoton microscopy. *Cancer Res*. 2014;74(10):2688-2697.
19. Lentsch G, Balu M, Williams J, et al. In vivo multiphoton microscopy of melasma. *Pigm Cell Melanoma Res*. 2019;32(3):403-411.
20. Huck V, Gorzelanny C, Thomas K, et al. From morphology to biochemical state - intravital multiphoton fluorescence lifetime imaging of inflamed human skin. *Sci Rep*. 2016;6:22789.
21. Lin J, Saknite I, Valdebran M, et al. Feature characterization of scarring and non-scarring types of alopecia by multiphoton microscopy. *Lasers Surg Med*. 2019;51(1):95-103.
22. Bazin R, Flament F, Colonna A, et al. Clinical study on the effects of a cosmetic product on dermal extracellular matrix components using a high-resolution multiphoton tomograph. *Skin Res Technol*. 2010;16(3):305-310.
23. König K, Raphael AP, Lin L, et al. Applications of multiphoton tomographs and femtosecond laser nanoprocessing microscopes in drug delivery research. *Adv Drug Del Rev*. 2011;63(4):388-404.
24. Darwin ME, Konig K, Kellner-Hoefer M, et al. Safety assessment by multiphoton fluorescence/second harmonic generation/hyper-Rayleigh scattering tomography of ZnO nanoparticles used in cosmetic products. *Skin Pharmacol Physiol*. 2012;25(4):219-226.
25. Ait El Madani H, Tancrede-Bohin E, Bensussan A, et al. In vivo multiphoton imaging of human skin: assessment of topical corticosteroid-induced epidermis atrophy and depigmentation. *J Biomed Opt*. 2012;17(2):026009.
26. Tancrede-Bohin E, Baldeweck T, Decencièrre E, et al. Non-invasive short-term assessment of retinoids effects on human skin in vivo using multiphoton microscopy. *J Eur Acad Dermatol Venereol*. 2015;29(4):673-681.
27. Mohammed YH, Holmes A, Haridass IN, et al. Support for the safe use of zinc oxide nanoparticle sunscreens: lack of skin penetration or cellular toxicity after repeated application in volunteers. *J Invest Dermatol*. 2019;139(2):308-315.
28. Alex A, Frey S, Angelene H, et al. In situ biodistribution and residency of a topical anti-inflammatory using fluorescence lifetime imaging microscopy. *Br J Dermatol*. 2018;179(6):1342-1350.
29. Timár F, Soós G, Szende B, Horváth A. Interdigitation index - A parameter for differentiating between young and older skin specimens. *Skin Res Technol*. 2000;6(1):17-20.
30. Wasserstein RL, Lazar NA. The ASA Statement on p-Values: Context, Process, and Purpose. *The American Statistician*. 2016;70(2):129-133.
31. Weiss JS, Ellis CN, Headington JT, Tincoff T, Hamilton TA, Voorhees JJ. Topical tretinoin improves photoaged skin. A double-blind vehicle-controlled study. *JAMA*. 1988;259(4):527-532.
32. Griffiths CE, Kang S, Ellis CN, et al. Two concentrations of topical tretinoin (retinoic acid) cause similar improvement of photoaging but different degrees of irritation. A double-blind, vehicle-controlled comparison of 0.1% and 0.025% tretinoin creams. *Arch Dermatol*. 1995;131(9):1037-1044.
33. Bhawan J, Olsen E, Lufrano L, Thorne EG, Schwab B, Gilchrist BA. Histologic evaluation of the long term effects of tretinoin on photodamaged skin. *J Dermatol Sci*. 1996;11(3):177-182.
34. Kafi R, Kwak HS, Schumacher WE, et al. Improvement of naturally aged skin with vitamin A (retinol). *Arch Dermatol*. 2007;143(5):606-612.
35. Bellemere G, Stamatias GN, Bruere V, Bertin C, Issachar N, Oddos T. Antiaging action of retinol: from molecular to clinical. *Skin Pharmacol Physiol*. 2009;22(4):200-209.
36. Randhawa M, Rossetti D, Leyden JJ, et al. One-year topical stabilized retinol treatment improves photodamaged skin in a double-blind, vehicle-controlled trial. *J Drugs Dermatol*. 2015;14(3):271-280.
37. Kong R, Cui Y, Fisher GJ, et al. A comparative study of the effects of retinol and retinoic acid on histological, molecular, and clinical properties of human skin. *J Cosmet Dermatol*. 2016;15(1):49-57.
38. Inoue Y, Hasegawa S, Yamada T, et al. Bimodal effect of retinoic acid on melanocyte differentiation identified by time-dependent analysis. *Pigment Cell Melanoma Res*. 2012;25(3):299-311.
39. Ortonne JP. Retinoic acid and pigment cells: a review of in-vitro and in-vivo studies. *Br J Dermatol*. 1992;127(Suppl 41), 43-47.
40. Yoshimura K, Tsukamoto K, Okazaki M, et al. Effects of all-trans retinoic acid on melanogenesis in pigmented skin equivalents and monolayer culture of melanocytes. *J Dermatol Sci*. 2001;27:68-75.
41. Griffiths CE, Russman AN, Majmudar G, Singer RS, Hamilton TA, Voorhees JJ. Restoration of collagen formation in photodamaged human skin by tretinoin (retinoic acid). *N Engl J Med*. 1993;329(8):530-535.
42. Fisher GJ, Datta S, Wang Z, et al. c-Jun-dependent inhibition of cutaneous procollagen transcription following ultraviolet irradiation is reversed by all-trans retinoic acid. *J Clin Invest*. 2000;106(5):663-670.
43. Varani J, Warner RL, Gharaee-Kermani M, et al. Vitamin A antagonizes decreased cell growth and elevated collagen-degrading matrix metalloproteinases and stimulates collagen accumulation in naturally aged human skin. *J Invest Dermatol*. 2000;114(3):480-486.

44. Fajuyigbe D, Lwin SM, Diffey BL, et al. Melanin distribution in human epidermis affords localized protection against DNA photodamage and concurs with skin cancer incidence difference in extreme phototypes. *FASEB J.* 2018;32(7):3700-3706.
45. Del Bino S, Sok J, Bessac E, Bernerd F. Relationship between skin response to ultraviolet exposure and skin color type. *Pigment Cell Res.* 2006;19(6):606-614.
46. Brenner M, Hearing VJ. The protective role of melanin against UV damage in human skin. *Photochem Photobiol.* 2008;84(3):539-549.

How to cite this article: Tancrede-Bohin E, Baldeweck T, Brizion S, et al. In vivo multiphoton imaging for non-invasive time course assessment of retinoids effects on human skin. *Skin Res Technol.* 2020;26:794–803. <https://doi.org/10.1111/srt.12877>